

Two Dicyanostilbene-Based Two-Photon Fluorescence Environmentally Sensitive Probes with Large Two-Photon Absorption Cross Sections and Two-Photon Triple Fluorescence

Chi-Bao Huang

School of Information Engineering, Zunyi Normal University, Zunyi, China

ABSTRACT

The unusually sensitive solvatochromism of 2,5-dicyano-4-methyl-4'-dimethylaminostilbene (1a) whose emission maximum varies from 445 nm in cyclohexane to 641 nm in DMSO are described. 1a with remarkably large two-photon cross sections exhibits very strong polarity-, viscosity-, and temperature-dependence of fluorescence, and can be used to detect polarities, viscosities, and temperature. The successful application of 1a provides a brilliant prototype for the developments of ideal two-photon fluorescence probes.

*Corresponding author

Chi-Bao Huang, School of Information Engineering, Zunyi Normal University, Zunyi 563002, China.

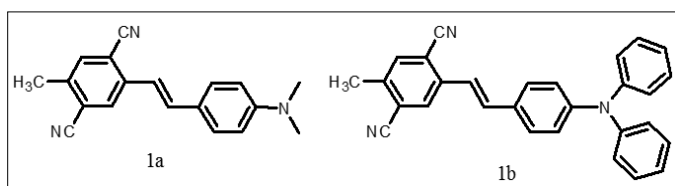
Received: January 23, 2023; Accepted: January 27, 2023; Published: February 28, 2023

For the development of TPEF (two-photon excited fluorescence)-optimized molecular probes, it is important to have a significant modulation of the photophysical properties of the chromophore in response to external stimuli, such as polarity, pH, ion concentration, and temperature. At the same time, the chromophore should retain a significant two-photon absorption (TPA) cross section (δ TPA) in a suitable excitation window for biological imaging (700-1000 nm, corresponding to an optimum combination of reduced scattering and absorption in biological samples). In contrast to PET-based fluorescence probes, which only show increasing or decreasing emission intensity at fixed wavelength, solvatochromic probes may indicate the presence of an analyte by a significant change of emission wavelength, which is unequivocally detectable [1]. However, at present, there are only a few examples of two-photon sensors for metal ions, fluoride ions, polarity, and pH that have been studied in organic solvents or model membranes [2,3]. Here we report on two dipolar dyes (1a-b) with two strongly electron-accepting cyano groups at their acceptor extremity derived from stilbene that display large changes in both one-(OPA) and TPA characteristics and solvatochromism which can be modulated by the addition of analytes. Surprisingly, these two probes exhibited reasonably large δ TPA, especially two-photon triple fluorescence.

1a exhibits an unexpected strong solvatochromism (Figure 1a, Supporting Information (SI)). Only a few previous examples of solvatochromic behavior for stilbene derivatives⁴ which just possess one substituent at most in the single aromatic ring and are not ideal candidates for solvatochromic probes had been reported. Thus, the emission maximum (EM) for 1a (1b) varies from 445 (452) nm in cyclohexane to 641 (604) nm in DMSO. The reason why the solvatochromic shifts of 1b are somewhat smaller (ca. 156 nm, cf. SI) is that decreasing transition energy and increasing sensitivity to solvent polarity for weak electron donor diphenylamino group is inferior to ones for strong electron donor dimethylamino group.

Table 1: Photophysical Properties of 1a

Solvent ^a	λ_{\max}^b	λ_{\max}^c	Φ^d	λ_{\max}^e	δ_{\max}^f
c-hexane	401	445	0.236	790	5560
toluene	405	510	0.504	790	2750
benzene	406	515	0.715	790	3150
dioxane	401	537	0.812	790	4480
THF	404	577	0.563	790	2820
CHCl ₃	404	554	0.456	790	3650
acetone	401	622	0.038	790	1120
DMF	402	634	0.112	790	130
DMSO	409	641	0.013	790	650
MeCN	396	632	0.019	790	980



The stilbene derivative 1a (1b) was obtained in 65% (62%) yield by the reaction of dimethylaminobenzaldehyde (diphenylaminobenzaldehyde) with (2,5-dicyano-4-methylbenzyl) phosphonic acid diethyl ester in the presence of sodium hydride (NaH). The absorption properties of 1a are almost independent on the solvent (Table 1). However, with respect to the emission properties,

a Solvents arranged in order of decreasing ET (30) value. b Absorption maximum with lowest energy in nm, c (1a) = 10⁻⁵ M. c Emission maximum in nm, c (1a) = 10⁻⁵ M, λ_{exc} = 410 nm. d Relative to quinine sulfate 10⁻⁶ M in 0.05 mol/L H₂SO₄; estimated error, $\pm 10\%$ of the given values. e Two-photon excitation maximum in nm. f The peak TPA cross-sections in 10⁻⁵⁰ cm⁴ s/photon (GM)

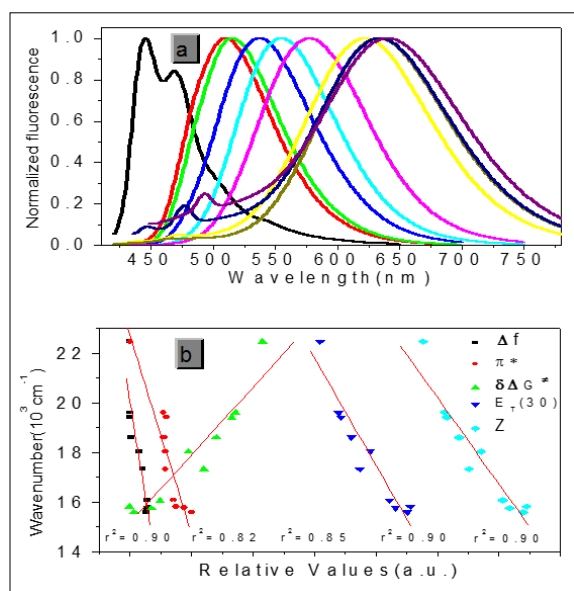


Figure 1: Normalized one-photon emission spectra (left to right: C-hexane, toluene, benzene, dioxane, CHCl_3 , THF, acetone, MeCN, DMF, DMSO) and (b) Correlation between the emission maxima (in cm^{-1}) of **1a** ($c = 10^{-5} \text{ M}$, $\lambda_{\text{ex}} = 410 \text{ nm}$) in various solvents and selected solvent parameters such as Δf , π^* , $\delta\Delta G^\ddagger$, $E_T(30)$ and Z.

Protic solvents (Hydrogen-Bonding-Donor, HBD) can interact with the donor (dimethylamino) for the ground state of **1a** to stabilize the ground state more than the excited state, and thus, lower energy for the ground state results in a relative blue shift as compared with strong polar aprotic solvents (Non-Hydrogen-Bonding-Donor, NHD). The fitting between EM in wavenumbers and the solvent parameters such as the $E_T(30)$ data, the Kosower parameter, Z, the Gibbs energy of activation of the solvolysis ($\delta\Delta G^\ddagger$), the index of solvent dipolarity/polarizability (π^*), Δf and the Lippert-Mataga scale (Δf) 7 gave an almost linear relationship ($r^2 = 0.90, 0.90, 0.90, 0.85, 0.82$, respectively) (Figure 1b). In one- and two-photon emissions (OPE and TPE), band A (1L_a) of **1a** in glycerol all shift to the red with increasing temperature, and the relative intensities of band B (1L_b) gradually decreases (Figure 2e, f). The viscosity dependence of the fluorescence for **1a** exhibits differences between A band and B band, and between OPE and TPE (Figure 2c, d). The intensities of B band in OPE and TPE steadily increase upon the augment of viscosities, whereas the intensities of A band in TPE at first rapidly decline, and then enhance, and a third band at 542 nm, namely exciplex (E) fluorescence from strong intermolecular donor-acceptor systems finally disappears in pure glycerol (Figure 2d). Never has this property in two-photon been reported. High viscosity preventing intermolecular charges from transfer should be responsible for the disappearance of the third band whose no emergence in the OPE possibly consists in its low intensity and short lifetime. In addition, at the low concentration (10^{-6} M) of **1a**, the intensity ratio (IR) I_a/I_b of the emission bands A and B decreases with increasing viscosity, but at the high concentration ($3 \times 10^{-6} \text{ M}$) the IR I_a/I_b increases, irrespective of OPE and TPE (cf. SI). Furthermore, concentration dependence^{8d} is found for the IR I_a/I_b of the emission bands A and B of **1a** in alcohol (cf. SI). The above environmental influences upon triple fluorescence bands A, B and E usually indicates three emissive species, i.e., the localized excited state (LE), a twisted intramolecular charge transfer state (TICT) and an intermolecular exciplex.

As expected, δTPA of **1a** climbs its maximum of 5560 GM in nonpolar cyclohexane, while in strongly polar aprotic DMF it falls to its minimum of 130 GM. In general, δTPA of **1a** are much larger in low polarity aprotic solvents than in high polarity aprotic solvents, which should be attributed to the excited state configuration transformation (Table 1). The reduction in emission intensity for **1a** in acetone and other more polar solvents together with a near lack of photoreactivity is certainly consistent with decay of the emissive state to one or more of the possible noncops-

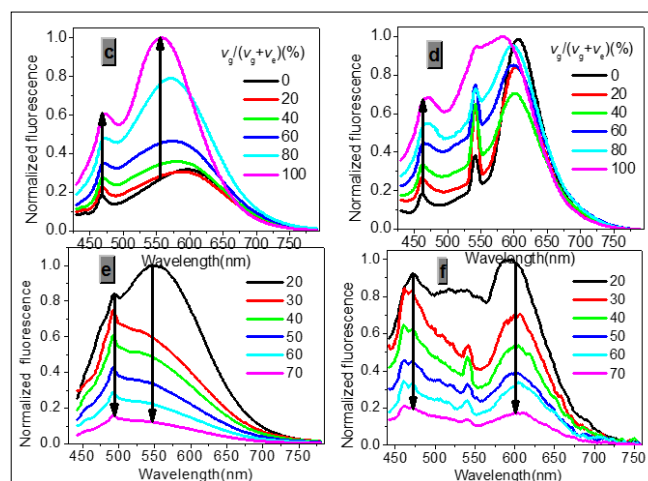


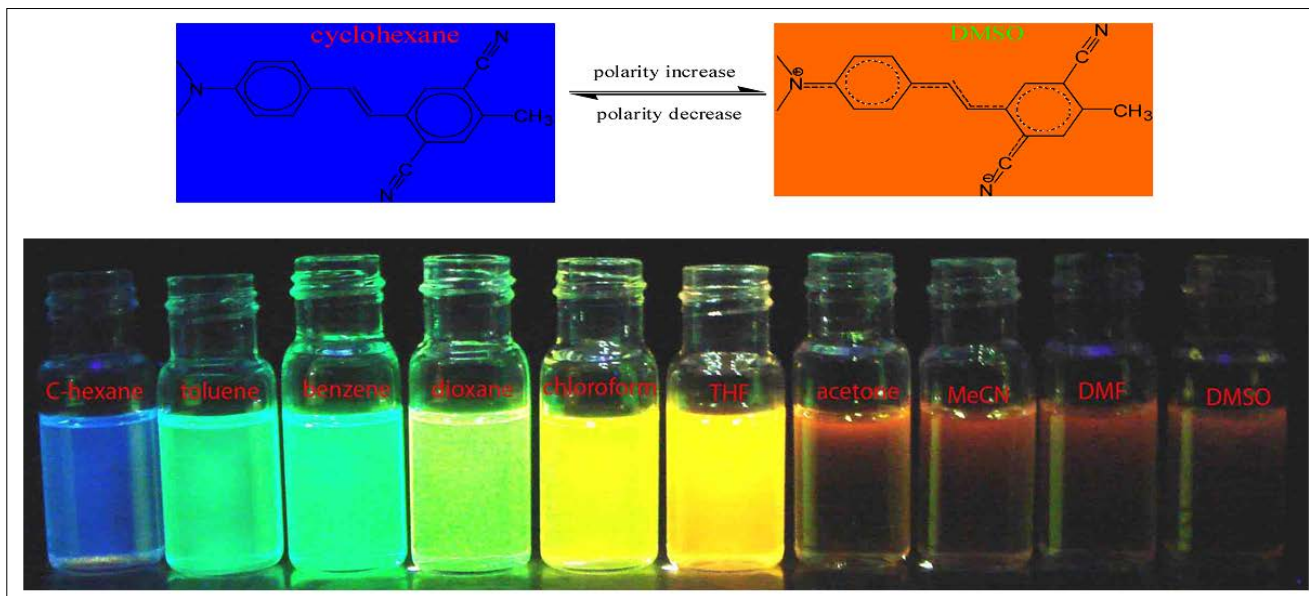
Figure 2: Normalized (c) one- and (d) two-photon emission spectra of **1a** ($c = 3 \times 10^{-6} \text{ M}$, $\lambda_{\text{ex}}(\text{OP}) = 410 \text{ nm}$, $\lambda_{\text{ex}}(\text{TP}) = 790 \text{ nm}$) in glycerol-ethanol ($v_g/(v_g+v_e)$, %). Normalized (e) one- and (f) two-photon emission spectra of **1a** ($c = 10^{-6} \text{ M}$, $\lambda_{\text{ex}}(\text{OP}) = 410 \text{ nm}$, $\lambda_{\text{ex}}(\text{TP}) = 790 \text{ nm}$) in glycerol versus temperature ($^\circ\text{C}$).

lanar and nonemissive TICT which subsequently decay rapidly to the ground state.

As in other solvatochromic systems,^{6d} an internal charge transfer (ICT) due to a strong donor-acceptor interplay between the dimethylamino and the 2,5-dicyano-4-methyl stilbyl moieties can take place in the excited state of **1a**. On one hand, ortho- and meta-cyano groups of double bonds ($\text{C}=\text{C}$) are fairly strong electron acceptor in the ground state, which can remarkably decrease transition energy, stabilize resonance structures and increase both the excited state dipole moment and molecular sensitivity to solvent polarity. On the other hand, these two cyano groups can notably extend conjugated system, which consumedly improves two-photon absorption cross section and fluorescence quantum yield. Additionally, in the excited state, the adiabatic ICT leads to an intermediate that most likely develops a negative charge for nitrogen atom of ortho-cyano group that is, after solvent relaxation,^{5, 6b, d} stabilized not only by polar solvents, especially those with high π^* , but also by meta-cyano group with strong electron-withdrawing ability for greater diffusion of concentrated negative charge. This ICT-solvent relaxation sequence explains the significant red shift of the emission spectra in polar solvents as well as the temperature and viscosity dependence of the emission properties.

In conclusion, we have shown that the covalent attachment of two cyano groups in the single aromatic ring and dimethylamino group to stilbene is a considerably ingenious strategy, which makes the molecule a highly sensitive two-photon thermo-solvatochromic probe with remarkably large δTPA and very high fluorescence quantum yield capable of being used to detect the analytes with high π^* , and to detect polarities, viscosities, and temperature. The

results provide a useful design strategy for synthesis of new two-photon sensors for further applications.



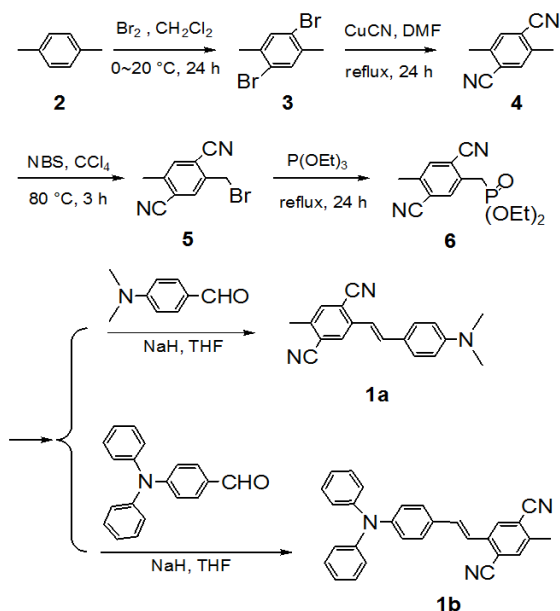
Supporting Information

Materials

NMR spectra were recorded on a VARIAN INOVA 400 MHz NMR spectrometer. Mass spectral determinations were made on a Q-TOF mass spectrometry (Micromass, England). High resolution mass spectra measurements were performed at a GC-TOF mass spectrometry (Micromass, US) (Electron Ionization source). Fluorescence measurements were performed on a PTI-C-700 Felix and Time-Master system. Fluorescence quantum yields were measured using standard methods on air-equilibrated samples at room temperature. Quinine bisulfate in 0.05M H₂SO₄ ($\Phi = 0.546$) was used as a reference. *TPEF* (two-photon-excited fluorescence) action cross-section spectra were measured according to the experimental protocol established by Xu and Webb, using a mode-locked Ti/sapphire laser that delivers ~ 80 fs pulses at 80 MHz. Fluorescein (10^{-4} M in 0.1M NaOH), whose *TPEF* action cross-sections are well-known, served as the reference. The quadratic dependence of the fluorescence intensity on the excitation intensity was verified for each data point, indicating that the measurements were carried out in intensity regimes in which saturation or photodegradation do not occur. The measurements were performed at room temperature on air-equilibrated solutions (10^{-5} M). The experimental uncertainty on the absolute action cross-sections determined by this method has been estimated to be $\pm 20\%$. Absorption spectra were measured on a HP-8453 spectrophotometer. Solvents were generally dried and distilled prior to use. Reactions were monitored by thin-layer chromatography on Merck silica gel 60 F₂₅₄ precoated aluminum sheets. Column chromatography: Merck silica gel Si 60 (40-63 μ m, 230-400 mesh).

Syntheses

2,5-dibromo-p-xylene(3), S3 2,5-dimethyl-terephthalonitrile(4), S3 4-(N,N-diphenyl amino)benzaldehyde, S4 were synthesized according to literature procedures.



2-Bromomethyl-5-methyl-terephthalonitrile (5)

2,5-dimethyl-terephthalonitrile (4) (2.0 g, 13 mmol), N-bromosuccinimide (NBS) (2.3 g, 13 mmol), benzoyl peroxide (BPO) (0.1 g) and CCl_4 (100 mL) were placed into a 250 mL flask, the mixture was refluxed for 2 h. After cooled to room temperature, the mixture was filtered, and the filtrate was concentrated by evaporating the solvent to get a viscous liquid. Flash chromatography on silica gel (20:1 CH_2Cl_2 :n-hexane) yielded the product as a white powder (1.9 g, 62%). $^1\text{H NMR}$ (CDCl_3 , 400 MHz) δ : 7.788 (s, 1H), 7.637 (s, 1H), 4.594 (s, 2H), 2.604 (s, 3H). HS-MS (EI) m/z : 233.9747 (calcd for $\text{C}_{10}\text{H}_7\text{BrN}_2$: 233.9793).

(2,5-Dicyano-4-Methylbenzyl)-Phosphonic Acid Diethyl Ester (6)

A solution of 2-Bromomethyl-5-methyl-terephthalonitrile (5) (1.4 g, 6 mmol) and $\text{P}(\text{OEt})_3$ (2.5 g, 15 mmol) in 10 mL toluene were heated to 120 °C for 5 h. Excess $\text{P}(\text{OEt})_3$ was removed in vacuo. Flash chromatography on silica gel (1:1 CH_2Cl_2 :ethyl acetate) yielded the product as a white crystalline solid (1.7 g, 98%). $^1\text{H NMR}$ (CDCl_3 , 400 MHz) δ : 7.758 (d, $J=2.8$ Hz, 1H), 7.619 (s, 1H), 4.133 (m, 4H), 3.377 (d, $J=22$ Hz, 2H), 2.580 (s, 3H), 1.312 (t, $J=7.2$ Hz, 6H). $^{13}\text{C NMR}$ (CDCl_3 , 400 MHz) δ : 141.267, 134.723, 134.662, 134.283, 117.416, 116.391, 62.929, 62.861, 32.672, 31.298, 20.102, 16.527, 16.466. HS-MS (EI) m/z : 292.0977 (calcd for $\text{C}_{14}\text{H}_{17}\text{N}_2\text{O}_3\text{P}$: 292.0977).

2,5-dicyano-4-methyl-4'-(dimethylamino)stilbene (1a).

Dimethylaminobenzaldehyde (170 mg, 1.14 mmol), and NaH (55 mg 2.28 mmol) were dissolved in 10 mL of tetrahydrofuran (THF), and the solution was cooled to 0 °C. To this solution, (2,5-dicyano-4-methylbenzyl)-phosphonic acid diethyl ester (6) (333 mg, 1.14 mmol) in 10 mL of THF was added dropwise, and the reaction mixture was stirred for 12 h at 0 °C. Water was added to the reaction mixture, and the product was extracted with ethyl acetate. The organic layer was dried with MgSO_4 followed by evaporation of the solvent. The crude product was separated by column chromatography with a gradient of hexane in dichloromethane (20-0%) and ethyl acetate in dichloromethane (0-20%). The resulting solid was recrystallized from acetone to give yellow powder (212 mg, 0.74 mmol, 65% in yield). m.p. 256-257 °C. $^1\text{H NMR}$ (CDCl_3 , 400 MHz) δ : 7.969 (s, 1H), 7.534 (s, 1H), 7.472 (d, $J=9.2$ Hz, 2H), 7.211 (d, $J=16$ Hz, 1H), 7.128 (d, $J=16$ Hz, 1H), 6.725 (d, $J=8.4$ Hz, 2H), 3.030 (s, 6H), 2.546 (s, 3H). $^{13}\text{C NMR}$ (CDCl_3 , 400 MHz) δ : 140.075, 139.050, 135.171, 134.404, 128.939, 128.802, 117.477, 117.105, 116.991, 113.902, 112.497, 40.567, 20.056. HS-MS (EI) m/z : 287.1326 (calcd for $\text{C}_{19}\text{H}_{17}\text{N}_3$: 287.1422).

2,5-dicyano-4-methyl-4'-(diphenylamino)stilbene (1b).

It is prepared by similar procedures given above for 1a. The crude product was purified by column chromatography on silica gel with dichloromethane-acetone (7:2) as eluent to give 1b in 62% yield as a green crystal. m.p. 213-214 °C. $^1\text{H NMR}$ (CDCl_3 , 400 MHz) δ : 7.977 (s, 1H), 7.567 (s, 1H), 7.424 (d, $J=7.6$ Hz, 2H), 7.310~7.258 (m, 5H), 7.234 (d, $J=19.6$ Hz, 1H), 7.120 (d, $J=16.4$ Hz, 1H), 7.121~7.039 (m, 5H), 2.565 (s, 3H). $^{13}\text{C NMR}$ (CDCl_3 , 400 MHz) δ : 147.271, 139.893, 139.521, 134.617, 134.496, 129.622, 129.129, 128.484, 125.303, 123.937, 122.570, 119.731, 117.598, 116.885, 114.387, 20.132. HS-MS (EI) m/z : 411.1697 (calcd for $\text{C}_{29}\text{H}_{21}\text{N}_3$: 411.1735).

Spectroscopy data

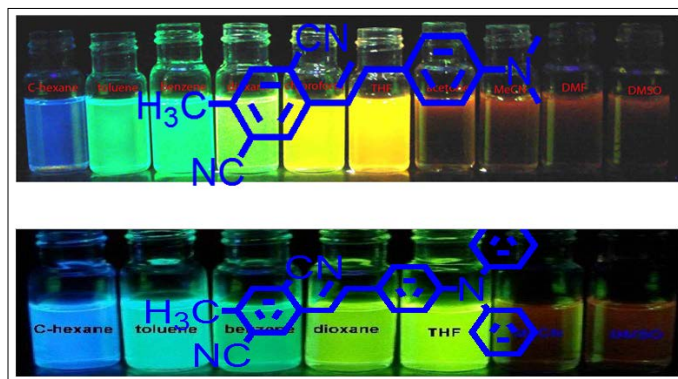


Figure S1: Picture of fluorescence of 1a and 1b ($c = 10^{-5}$ M, $\lambda_{\text{ex}} = 365$ nm) in different solvents.

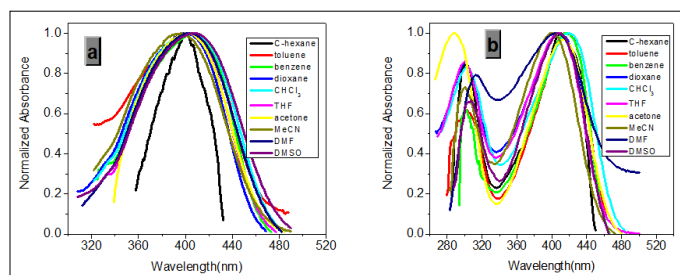


Figure S2: Normalized absorption spectra of 1a (a) and 1b (b) ($c = 10^{-5}$ M) in various solvents

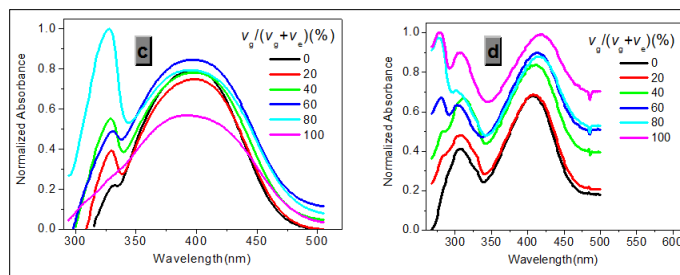


Figure S3: Normalized absorption spectra of 1a (c) and 1b (d) ($c = 10^{-5}$ M) in glycerol-ethanol ($v_g/(v_g+v_e)$, %).

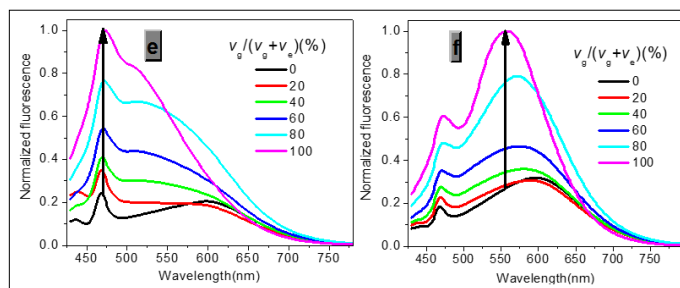


Figure S4: Normalized one-photon emission spectra of 1a ((e) $c = 10^{-6}$ M, (f) $c = 3 \times 10^{-6}$ M, $\lambda_{\text{ex}} = 410$ nm) in glycerol-ethanol ($v_g/(v_g+v_e)$, %).

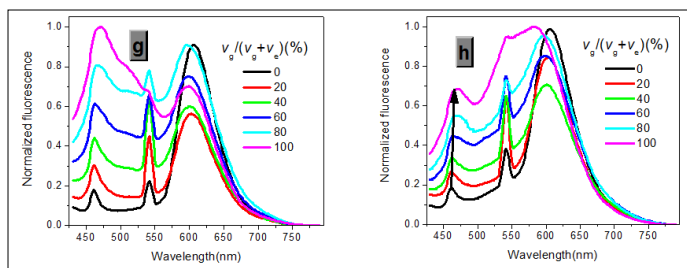


Figure S5: Normalized two-photon emission spectra of 1a ((g) $c = 10^{-6}$ M, (h) $c = 3 \times 10^{-6}$ M, $\lambda_{ex} = 790$ nm) in glycerol-ethanol ($v_g/(v_g+v_e)$, %).

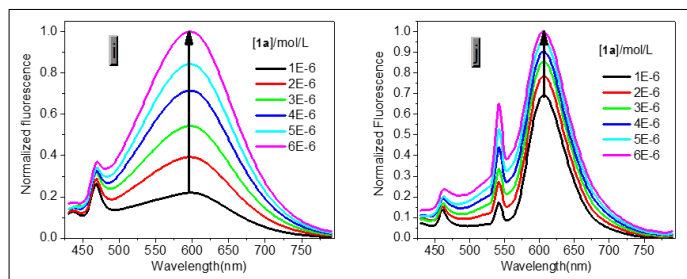


Figure S6: Normalized (i) one- ($\lambda_{ex} = 410$ nm) and (j) two-photon ($\lambda_{ex} = 790$ nm) emission spectra of 1a in ethanol versus its concentrations.

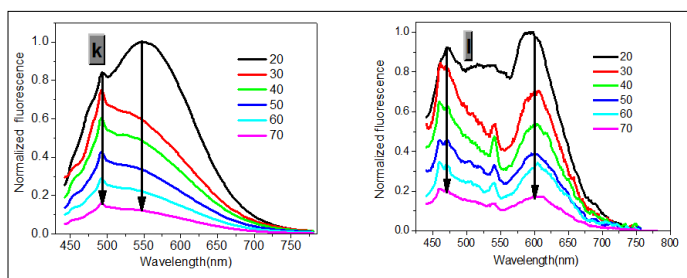


Figure S7: Normalized (k) one- ($\lambda_{ex} = 410$ nm) and (l) two-photon ($\lambda_{ex} = 790$ nm) emission spectra of 1a ($c = 10^{-6}$ M) in glycerol versus temperature ($^{\circ}$ C).

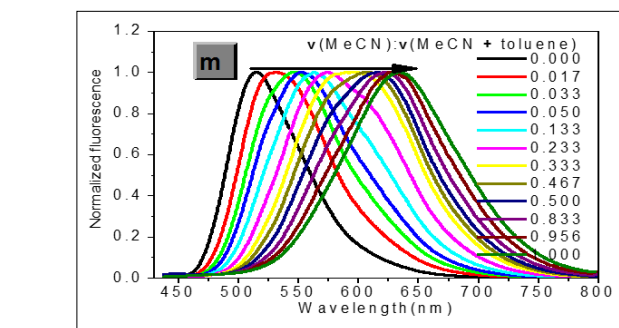


Figure S8: Normalized one-photon emission spectra of 1a ($c = 10^{-5}$ M, $\lambda_{ex} = 410$ nm) in toluene-MeCN mixture versus MeCN concentrations

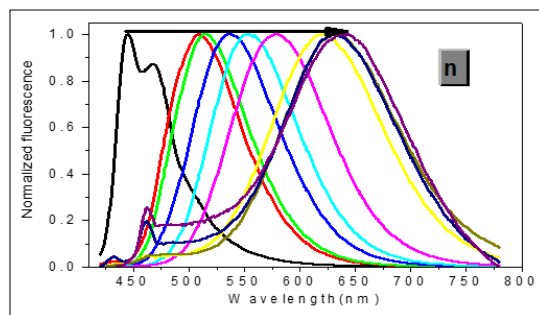


Figure S9: Normalized two-photon emission spectra (left to right: C-hexane, toluene, benzene, dioxane, $CHCl_3$, THF, acetone, MeCN, DMF, DMSO) of 1a ($c = 10^{-5}$ M, $\lambda_{ex} = 790$ nm) in various solvents.

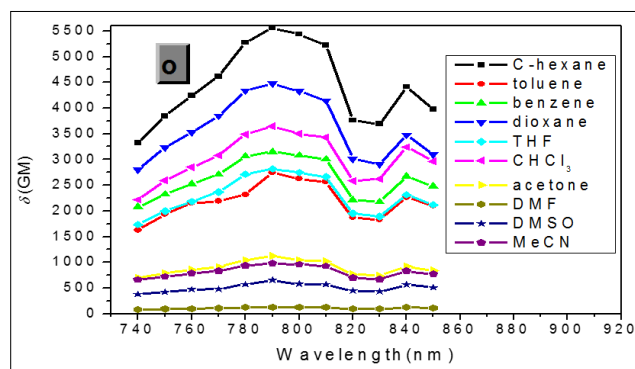


Figure S10: Two-photon absorption cross sections of 1a ($c = 10^{-5}$ M) in various solvents versus two-photon excited wavelengths

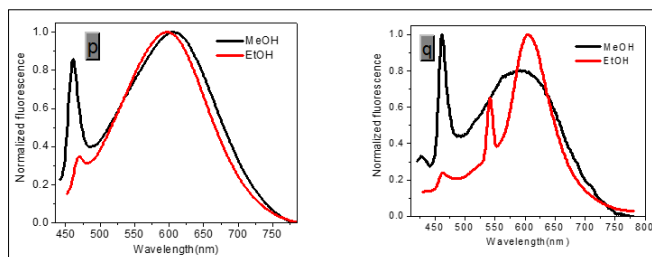


Figure S11: Normalized (p) one- ($\lambda_{ex} = 410$ nm) and (q) two-photon ($\lambda_{ex} = 790$ nm) emission spectra of 1a ($c = 10^{-5}$ M) in MeOH and EtOH. One-photon emission maxima in MeOH and EtOH are 605 and 597 nm respectively.

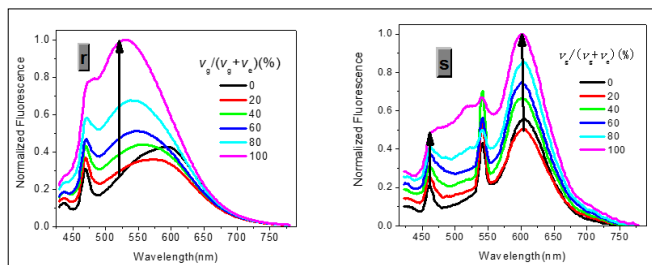


Figure S12: Normalized (r) one- ($\lambda_{ex} = 412$ nm) and (s) two-photon ($\lambda_{ex} = 810$ nm) emission spectra of 1b ($c = 10^{-6}$ M) in glycerol-ethanol ($v_g/(v_g+v_e)$, %).

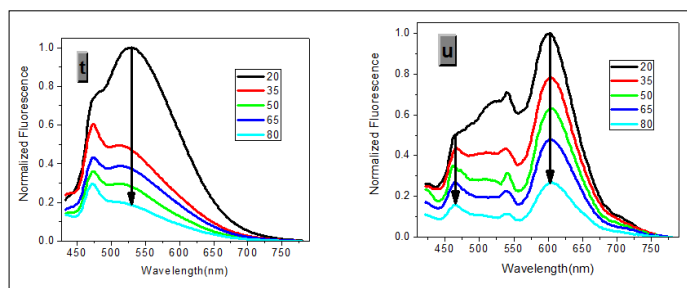


Figure S13: Normalized (t) one- ($\lambda_{ex} = 410$ nm) and (u) two-photon ($\lambda_{ex} = 790$ nm) emission spectra of **1b** ($c = 10^{-6}$ M) in glycerol versus temperature ($^{\circ}\text{C}$).

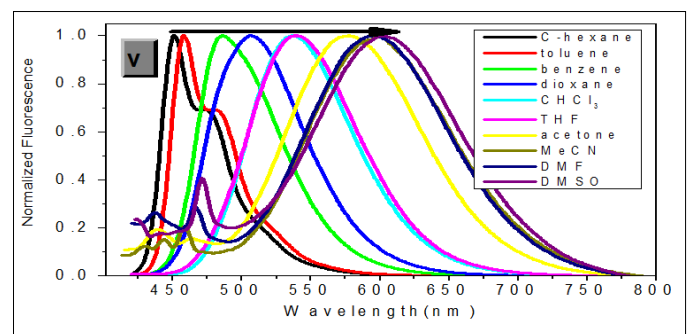


Figure S14: Normalized one-photon emission spectra of **1b** ($c = 10^{-6}$ M, $\lambda_{ex} = 412$ nm) in various solvents

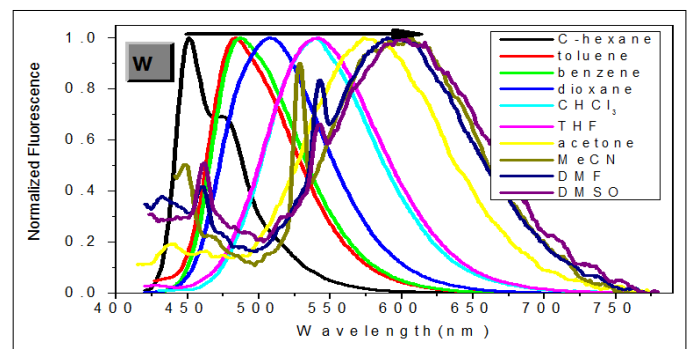


Figure S15: Normalized two-photon emission spectra of **1b** ($c = 10^{-6}$ M, $\lambda_{ex} = 810$ nm) in various solvents

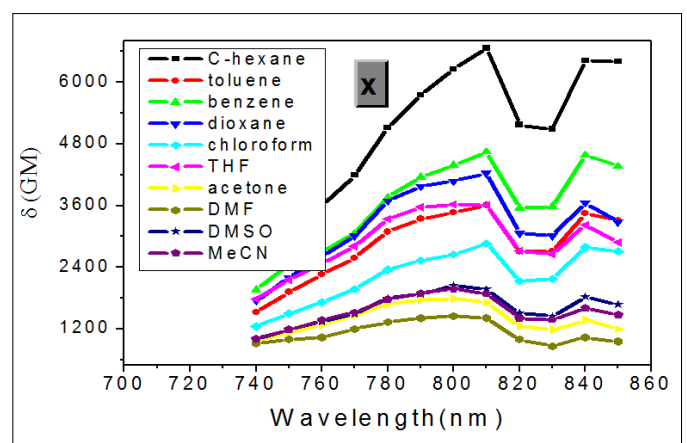


Figure S16: Two-photon absorption cross sections of **1b** ($c = 10^{-6}$ M) in various solvents versus two-photon excited wavelengths

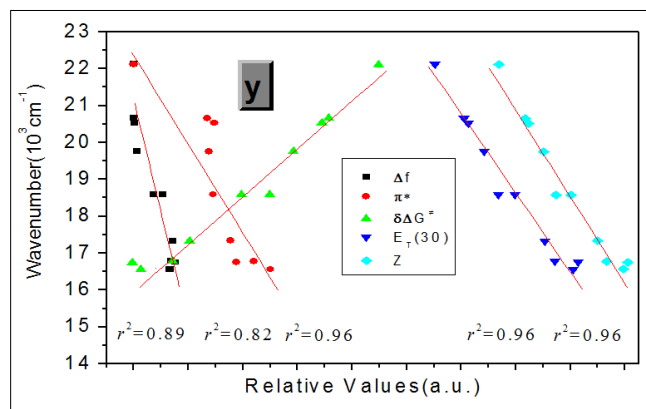


Figure S17: Correlation between the emission maxima (in cm^{-1}) of **1b** ($c = 10^{-6}$ M, $\lambda_{ex} = 412$ nm) in various solvents and selected solvent parameters such as Δf , π^* , $\delta\Delta G^{\ddagger}$, $E_T(30)$ and Z .

Table S18: Photophysical Properties of 1b

Solvent ^a	$\lambda_{max}^{(1)}$ ^b	$\lambda_{max}^{(2)}$ ^c	$\Phi_{em}^{(1)}$ ^d	$\lambda_{max}^{(2)}$ ^e	$\delta_{max}^{(f)}$
c-hexane	410	451	0.805	810	6670
toluene	416	458	0.814	810	3610
benzene	416	486	0.846	840	4650
dioxane	410	507	0.885	810	4230
THF	407	539	0.763	810	3720
CHCl_3	419	537	0.745	840	2860
acetone	413	578	0.265	800	1790
DMF	405	595	0.106	800	1450
DMSO	410	603	0.066	800	1980
MeCN	401	599	0.058	800	2040

^a Solvents arranged in order of decreasing $E_T(30)$ value. ^b Absorption maximum with lowest energy in nm, $c(\mathbf{1b}) = 10^{-5}$ M. ^c Emission maximum in nm, $c(\mathbf{1b}) = 10^{-6}$ M, $\lambda_{ex} = 412$ nm. ^d Relative to quinine sulfate 10^{-6} M in 0.05 mol/L H_2SO_4 ; estimated error, $\pm 5\%$ of the given values. ^e Two-photon excitation maximum in nm. ^f The peak TPA cross-sections in 10^{-50} $\text{cm}^4/\text{s/photon}$ (GM)

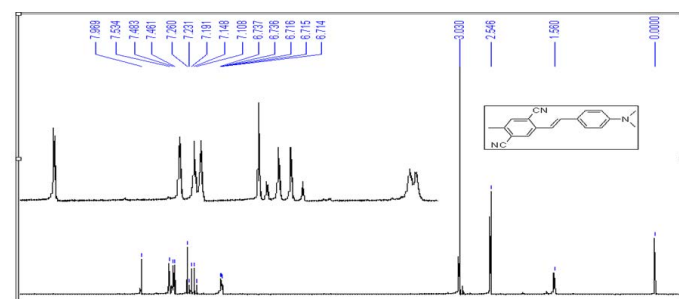


Figure S19: ^1H NMR spectrum for probe **1a**

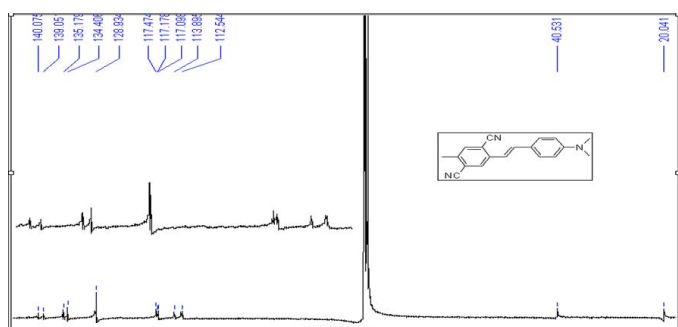


Figure S20: ^{13}C NMR spectrum for probe **1a**

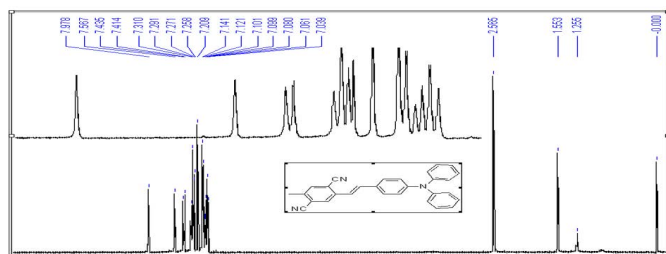


Figure S21: ^1H NMR spectrum for probe **1b**

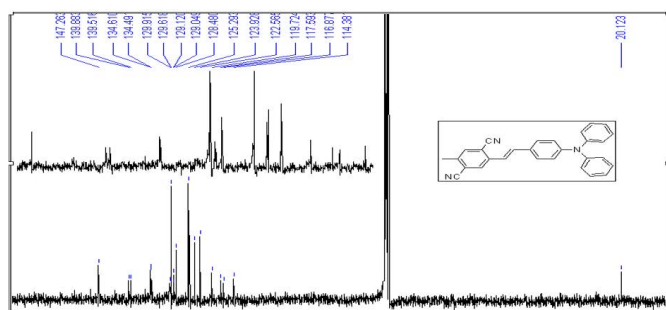


Figure S22: ^{13}C NMR spectrum for probe **1b**

Acknowledgment: This work was supported by the Ministry of Education of China and National Natural Science Foundation of China (project 20128005, 20376010 and 20472012).

Supporting Information Available: Synthetic details and other spectroscopy data. This material is available free of charge via the Internet at <http://pubs.acs.org>.

References

- (S1) Eaton DF (1988) *J Photochem. Photobiol B* 2: 523-531.
 (S2) Xu C, Webb WWJ (1996) *Opt. Soc. Am. B* 13: 481-491.
 (S3) Huang H, He Q, Lin H (2004) *Polym. Adv. Technol* 15: 84.
 (S4) Baker TN III, Doherty WP Jr, Kelley WS, Newmeyer W, Rogers JE Jr, et al (1965) *Org. Chem.* 30 3714-3718.
- Bohne C, Ihmels H, Waidelich M, Yihwa C (2005) N-Acylureido Functionality as Acceptor Substituent in Solvatochromic Fluorescence Probes: Detection of Carboxylic Acids, Alcohols, and Fluoride Ions. *J. Am. Chem. Soc* 127: 17158.
 (a) Pond SJK, Tsutsumi O, Rumi M, Kwon O, Zojer E, et al. (2004) Metal-Ion Sensing Fluorophores with Large Two-Photon Absorption Cross Sections: Aza-Crown Ether Substituted Donor-Acceptor-Donor Distyrylbenzenes. *J. Am. Chem. Soc* 126: 9291.
 (b) Kim HM, Jeong MY, Ahn HC, Jeon SJ, Cho BR (2004) Two-Photon Sensor for Metal Ions Derived from Azacrown

Ether J. Org. Chem 69: 5749-5751.

- (c) Ahn HC, Yang SK, Kim HM, Li S, Jeon S-J, et al. (2005) *Chem. Phys. Lett.* 410, 312.
 (d) Kim JS, Kim HJ, Kim HM, Kim SH, Lee JW, et al. (2006) Cho, B. R. *J. Org. Chem* 71: 8016.
- (a) Werts MHW, Gmouh S, Mongin O, Pons T, Blanchard-Desce M (2004) Strong Modulation of Two-Photon Excited Fluorescence of Quadripolar Dyes by (De)Protonation. *J Am Chem Soc* 126: 16294-16295.
 (b) Liu Z-Q, Shi M, Li F-Y, Fang Q, Chen Z-H, et al. (2005) Highly Selective Two-Photon Chemosensors for Fluoride Derived from Organic Boranes. *Org Lett* 7: 5481- 5484.
 (c) Kim HM, Yang HJ, Kim PR, Seo MS, Yi J-S, et al. (2007) Magnesium Ion Selective Two-Photon Fluorescent Probe Based on a Benzo[h]chromene Derivative for in Vivo Imaging. *Cho B R J Org Chem* 72: 2088- -2096.
 (d) Droumaguet CL, Mongin O, Werts MHV, Blanchard-Desce M (2005) Towards "smart" multiphoton fluorophores: strongly solvatochromic probes for two-photon sensing of micropolarity. *Chem Commun* 2005: 2802-2804.
- (a) Bent DV, Sohulte-Frohlinde DJ, *Phys. Chem.* 1974, 28, 446.
 (b) Schanze KS, Shin DM, Whitten DG (1985) *J. Am. Chem. Soc.* 107: 507.
 (c) Shin DM, Whitten DG (1988) Solvatochromic behavior of intramolecular charge-transfer diphenylpolyenes in homogeneous solution and microheterogeneous media *J. Phys. Chem.* 1988, 92, 2945.
 (d) Lewis FD, Sinks LE, Weigel W, Sajimon MC, Crompton EM *J. Phys. Chem. A* 109: 2443- 2956.
 (e) Jager WF, Volkers AA, Neckers DC (1995) *Macromolecules* 28: 8153.
- Reichardt C (1994) Solvatochromic Dyes as Solvent Polarity Indicators. *Chem. Rev.* 94: 2319- 2358.
- (a) Kbamlet MJ, Abboud J-LM, Taft R (1981) An Examination of Linear Solvation Energy Relationships *W. Prog. Phys. Org. Chem* 13: 485.
 (b) Retting W *Angew* (1986) Charge Separation in Excited States of Decoupled Systems—TICT Compounds and Implications Regarding the Development of New Laser Dyes and the Primary Process of Vision and Photosynthesis *Chem. Int. Ed. Eng* 971.
 (c) Collins GE, Choi L-S, Callahan JH (1998) *J. Am. Chem. Soc* 120: 1474.
 (d) Kamlet MJ, Abboud JL, Taft RW (1977) The solvatochromic comparison method. 6. The .pi.* scale of solvent polarities. *J. Am. Chem. Soc* 99: 6027- 6038.
- (a) Lippert EZ, *Naturforsch A* (1955) 10: 541.
 (b) Mataga N, Kaifu Y, Koizumi M *Bull* (1956) Solvent Effects upon Fluorescence Spectra and the Dipolemoments of Excited Molecules. *Chem Soc Jpn* 29: 465.
- (a) Knibbe H, Rollig K, Schifer FP, Weller AJ (1957) *Chem. Phys* 47: 1184.
 (b) Knibbe H, Rehm D, Weller A *Ber, Bunsen-Ges* (1968) *Phys Chem* 72: 257.
 (c) Weller, A. Z (1982) Photoinduced Electron Transfer in Solution: Exciplex and Radical Ion Pair Formation Free Enthalpies and their Solvent Dependence. *Phys. Chem. (Wiesbaden)* 133: 93.
 (d) Khalil OS (1975) *Chem Phy Lett* 35: 172.

Copyright: ©2023 Chi-Bao Huang. This is an open-access article distributed under the terms of the Creative Commons Attribution License, which permits unrestricted use, distribution, and reproduction in any medium, provided the original author and source are credited.